

Calculation of electron-lithium scattering using the coupled-channel optical method

Igor Bray,* Dmitry V. Fursa, and Ian E. McCarthy

*Electronic Structure of Materials Centre, School of Physical Sciences, The Flinders University of South Australia,
G.P.O. Box 2100, Adelaide 5001, Australia*

(Received 7 August 1992)

We present calculations of spin asymmetries for the elastic and 2^2P channels, differential and integrated cross sections for the elastic through to 4^2F channels, and total cross sections of electrons scattering on lithium at a range of energies from 1 to 200 eV. Very good agreement is found with available measurements at all energies, which for the spin asymmetries may only be achieved by the inclusion of coupling of the low-lying target states to the target continuum.

PACS number(s): 34.80.Bm, 34.80.Dp, 34.80.Nz

I. INTRODUCTION

Calculation of electron-atom scattering is of fundamental interest to a theorist. One-electron atoms, e.g., hydrogen and the alkali metals, provide an ideal testing ground for many theories. The hydrogen atom is most ideal for the theorist as its wave functions are known exactly. However, atomic hydrogen is a difficult target for experimentalists, but the alkali metals present fewer problems. These hydrogenlike atoms are well modeled by the Hartree-Fock model of one valence electron above a frozen core, particularly for the lighter alkali metals. As a result there is a considerable amount of data of electron scattering on alkali metals which may be used to thoroughly test any scattering theory.

The coupled-channel optical (CCO) formalism of Bray, Konovalov, and McCarthy [1] has proved to be one of the most successful theories of electron-atom scattering to date. It is based on the close-coupling formalism, but in addition is able to treat the target continuum states via a complex nonlocal polarization potential. It is therefore applicable at all projectile energies, which has been amply verified by comparison with experimental differential cross sections for hydrogen [1, 2] and sodium [3, 4]. Bray [5] showed that the treatment of the target continuum had a very large effect on the sodium spin asymmetries at projectile energies of 10 and 20 eV, and yielded excellent agreement with experiment. A full application of the method by Bray and McCarthy [6] to electron-sodium scattering data of Celotta and co-workers [7–11] and Hegemann *et al.* [12] showed that it was applicable to spin-dependent data at a range of projectile energies from 1 to 40 eV. As a result, this work demonstrated that in describing scattering phenomena, electron-sodium scattering may be treated as a three-body problem of a frozen core with one valence electron and one projectile electron. Thus the relatively simple theory of electron-hydrogen scattering may be directly applied to electron-sodium scattering with the interchange of the electron-proton potential of hydrogen for the frozen-core Hartree-Fock potential of sodium.

The aim of this paper is to apply the CCO formalism to lithium. We do this with a number of purposes in mind. The nature of the spin asymmetry data for lithium of Baum and co-workers [13, 14] is different from that of Celotta's group. Rather than presenting differential spin asymmetries at each energy, Baum and co-workers measured the spin asymmetry at three angles as a function of the energy of the incident projectile electron. This allows for a test of the theory at a continuous range of energies which may be used, for example, to establish at which energy continuum states become important. An important feature of the CCO method is that the T -matrix elements for the transition from the ground state to any of the discrete target states, treated via the close-coupling formalism, are simultaneously calculated. This allows us to compare with available measurements the differential cross section of higher, as well as lower, excited states resulting from a single calculation, and we do so in this work.

There have been a number of electron-atom scattering theories applied to electron-lithium scattering with various degrees of success. The close-coupling calculations of Burke and Taylor [15] and Moores [16] yield good results for low projectile energies, though they do not attempt to study convergence as a function of the number of target states treated in the close-coupling formalism. Some higher-energy approximations based on perturbative approaches have been applied by Kumar, Tayal, and Tripathi [17] and Gien [18]. Mathur and Purohit [19] applied a two-potential approach, also to higher energies. None of these theories is able to reproduce the data of Baum and co-workers [13, 14] in the intermediate energy region. We shall see that our CCO method works equally well in all energy regions.

In Sec. II we give the formal derivation of the CCO equations for electron scattering on one-electron targets. This combines the ideas of an earlier work [1], where use of symmetric Feshbach projection operators P and Q was introduced, together with the fact that the three-body scattering problem has core states for nonhydrogen one-electron targets.

In Secs. III and IV we present the results of our CCO calculations which have been performed at a range of pro-

jectile energies of 1 to 200 eV incident on the ground state of lithium. We compare our results with measurements of the elastic and 2^2P spin asymmetries and differential cross sections, as well as the differential cross sections of the 3^2S , $3^2P + 3^2D$ and $4^2P + 4^2D + 4^2F$ channels.

II. THEORY

In order to calculate electron scattering on one-electron atoms we make the approximation that the complete problem may be treated as a three-body problem. The interacting particles are taken to be the frozen core and the valence and projectile electrons. Thus, we write the total Hamiltonian of the system as

$$H = H_1 + H_2 + V_{12}, \quad (1)$$

where

$$H_\alpha = K_\alpha + V_\alpha \quad (2)$$

is the one-electron Hamiltonian for both the projectile ($\alpha = 1$) and the valence ($\alpha = 2$) electrons. The electron-electron potential is V_{12} , and the potential of the core in the space denoted by α is V_α .

To define V_α we first find the one-electron core wave functions $|\phi_j\rangle \in C$ by solving the self-consistent-field Hartree-Fock equations [20] for the ground state of the target atom. We use these wave functions to define the frozen-core Hartree-Fock potential to which we may also add a phenomenological core-polarization potential. To obtain the set of one-electron noncore target states $|\phi_j\rangle \notin C$, discrete and continuous orthogonalized to the core states, we solve [21]

$$(K_2 + V_2 - \varepsilon_j) \phi_j(\mathbf{r}) = 0, \quad \phi_j \notin C \quad (3)$$

where

$$\begin{aligned} V_2 \phi_j(\mathbf{r}) = & \left(-\frac{Z}{r} + v_{\text{pol}}(r) \right. \\ & \left. + 2 \sum_{\phi_{j'} \in C} \int d^3r' \frac{|\phi_{j'}(\mathbf{r}')|^2}{|\mathbf{r} - \mathbf{r}'|} \right) \phi_j(\mathbf{r}) \\ & - \sum_{\phi_{j'} \in C} \int d^3r' \frac{\phi_{j'}^*(\mathbf{r}') \phi_j(\mathbf{r}')}{|\mathbf{r} - \mathbf{r}'|} \phi_{j'}(\mathbf{r}). \end{aligned} \quad (4)$$

We use the form of the polarization potential v_{pol} given by Zhou *et al.* [22]:

$$v_{\text{pol}}(r) = \frac{-\alpha}{2r^4} \{1 - \exp[-(r/\rho)^6]\}, \quad (5)$$

where α is the static dipole polarizability constant [23], and ρ is determined by trial and error to get the best possible one-electron energies. Note that the same values of α and ρ apply for all partial waves of $|\phi_j\rangle$. For lithium we take $\alpha = 0.19a_0^3$ and $\rho = 1.4a_0$, see Table I. Having good one-electron energies is important when the incident electron energy is near a threshold for excitation of one of the inelastic states. Furthermore, Bray and

TABLE I. Ionization energies (eV) of the lithium states used in the 13CC and 13CCO8 calculations. The pure frozen-core Hartree-Fock results are denoted by FCHF. The results with an added phenomenological polarization potential given in Eq. (5), with $\alpha = 0.19a_0^3$ and $\rho = 1.4a_0$, are denoted by FCHF⁺. The experimental values are due to Moore [31].

State	FCHF	FCHF ⁺	Experiment
2s	5.342	5.391	5.390
3s	2.008	2.018	2.018
4s	1.047	1.051	1.050
5s	0.641	0.643	0.643
2p	3.500	3.538	3.545
3p	1.545	1.555	1.557
4p	0.864	0.869	0.870
5p	0.552	0.554	0.554
3d	1.512	1.513	1.513
4d	0.850	0.851	0.851
5d	0.544	0.544	0.544
4f	0.850	0.850	0.850
5f	0.544	0.544	0.543

McCarthy [6] have shown that this potential results in a small, but significant improvement in agreement between theory and experiment for the sodium L_\perp parameters.

Having defined the structure of the atom we are now in a position to solve the three-body Schrödinger equation

$$(E - H)|\Psi^S\rangle = 0, \quad (6)$$

where S is the total spin ($S = 0, 1$ for singlet, triplet scattering, respectively). In the CCO formalism the difficulty of treating the target continuum is relegated to a complex nonlocal polarization potential which is derived using the Feshbach projection operators P and Q . For nonhydrogen one-electron atoms this procedure must be performed taking into account the existence of core states.

We use the complete set of target states to define the projection operators I_α , C_α , \bar{C}_α , P_α , Q_α , via

$$\begin{aligned} I_\alpha &= \sum_{\phi_i \in I_\alpha} |\phi_i\rangle \langle \phi_i| \\ &= \sum_{\phi_i \in C_\alpha} |\phi_i\rangle \langle \phi_i| + \sum_{\phi_i \in P_\alpha} |\phi_i\rangle \langle \phi_i| + \int_{\phi_i \in Q_\alpha} |\phi_i\rangle \langle \phi_i| \\ &= C_\alpha + P_\alpha + Q_\alpha \quad (\text{respectively}) \\ &= C_\alpha + \bar{C}_\alpha \end{aligned} \quad (7)$$

for $\alpha = 1, 2$. Here the target space has been split into a finite sum over the core states, an infinite sum over the discrete noncore states, and an integral over the continuum states. We define orthogonal symmetric P and Q projection operators by

$$P = P_1 \bar{C}_2 + \bar{C}_1 P_2 - P_1 P_2, \quad Q = Q_1 Q_2. \quad (8)$$

With this definition it can be simply verified that $P+Q = \bar{C}_1 \bar{C}_2$. As the core is completely filled the total wave function $|\Psi^S\rangle$ must be orthogonal to the core states, i.e.,

$$|\Psi^S\rangle = \bar{C}_1 \bar{C}_2 |\Psi^S\rangle = (P + Q)|\Psi^S\rangle. \quad (9)$$

Projecting (6) by P , then Q , together with (9) we have the P -projected Schrödinger equation

$$P(E - H - V_Q)P|\Psi^S\rangle = 0, \quad (10)$$

where

$$PV_Q P = PHQ \frac{1}{Q(E - H)Q} QHP \quad (11)$$

is the Feshbach complex nonlocal polarization potential.

Due to the Pauli exclusion principle the total wave function must satisfy the symmetry property

$$|\Psi^S\rangle = (-1)^S P_r |\Psi^S\rangle, \quad (12)$$

where we use P_r to denote the space exchange operator. Using (12) we can write

$$\begin{aligned} P|\Psi^S\rangle &= \frac{1}{2}[1 + (-1)^S P_r](\bar{C}_1 + Q_1)P_2|\Psi^S\rangle \\ &= \frac{1}{2}[1 + (-1)^S P_r]P_2|\psi^S\rangle, \end{aligned} \quad (13)$$

where we define

$$P_2|\psi^S\rangle = (\bar{C}_1 + Q_1)P_2|\Psi^S\rangle. \quad (14)$$

To solve the P -projected Schrödinger equation (10) we first employ the multichannel expansion

$$P_2|\psi^S\rangle = \sum_{\phi_i \in P_2} |\phi_i f_i^S\rangle, \quad (15)$$

where the $|f_i^S\rangle = \langle \phi_i | \psi^S \rangle$ are functions which by (12) and (14) for $|\phi_j\rangle \in P_1$ must satisfy

$$\langle \phi_i | f_j^S \rangle = (-1)^S \langle \phi_j | f_i^S \rangle. \quad (16)$$

Bray and Stelbovics [24] have shown that without this condition the $|f_i^S\rangle$ would not be uniquely defined. Substituting (13) in (10), and projecting with P_2 ($P_2 P = P_2$) we obtain

$$\begin{aligned} P_2(E - K_1 - H_2)P_2|\psi^S\rangle &= P_2 \{V_1 + (V_{12} + V_Q)[1 + (-1)^S P_r] - (-1)^S (E - H_1 - H_2)P_r\} P_2|\psi^S\rangle \\ &= P_2 \{V_1 + (V_{12} + V_Q)[1 + (-1)^S P_r] - P_1(E - H_1 - H_2)\} P_2|\psi^S\rangle \\ &= P_2 V_Q^S P_2 |\psi^S\rangle, \end{aligned} \quad (17)$$

which defines V_Q^S , and where we imposed the symmetry condition (16) by considering for $\langle \phi_j | \in P_2$

$$\begin{aligned} (-1)^S \langle \phi_j | (E - H_1 - H_2)P_r P_2 |\psi^S\rangle &= (-1)^S \sum_{\phi_i \in P_1} (E - H_1 - \varepsilon_j) |\phi_i\rangle \langle \phi_j | f_i^S \rangle \\ &= \sum_{\phi_i \in P_1} (E - H_1 - \varepsilon_j) |\phi_i\rangle \langle \phi_i | f_j^S \rangle \\ &= \langle \phi_j | P_1 (E - H_1 - H_2) P_2 |\psi^S\rangle. \end{aligned} \quad (18)$$

This is the simplest way of imposing condition (16). It is also imposed by writing

$$(-1)^S \langle \phi_j | f_i^S \rangle = (-1)^S (1 - \theta) \langle \phi_j | f_i^S \rangle + \theta \langle \phi_i | f_j^S \rangle \quad (19)$$

for any nonzero θ . This introduces an arbitrary constant into the equations, yet we find that the results are independent of θ , and so it is convenient to set it to unity for simplicity of presentation.

The asymptotic states $|\phi_i \mathbf{k}\rangle$ are solutions of

$$P_2(E - K_1 - H_2)P_2|\phi_i \mathbf{k}\rangle = 0. \quad (20)$$

For projectile $|\mathbf{k}_0\rangle$ incident on the target in state $|\phi_0\rangle$ we have the on-shell energy $E = k_0^2/2 + \varepsilon_0$. As the P_2 -projected T matrix is given by

$$\langle \mathbf{k} \phi_i | T^S | \phi_0 \mathbf{k}_0 \rangle = \langle \mathbf{k} \phi_i | V_Q^S P_2 |\psi^S(\phi_0, \mathbf{k}_0)\rangle, \quad (21)$$

using (17) we have the Lippmann-Schwinger equation

$$\langle \mathbf{k} \phi_i | T^S | \phi_0 \mathbf{k}_0 \rangle = \langle \mathbf{k} \phi_i | V_Q^S | \phi_0 \mathbf{k}_0 \rangle + \sum_{\phi_{i'} \in P} \int d^3 k' \frac{\langle \mathbf{k} \phi_i | V_Q^S | \phi_{i'} \mathbf{k}' \rangle}{(E + i0 - \varepsilon_{i'} - k'^2/2)} \langle \mathbf{k}' \phi_{i'} | T^S | \phi_0 \mathbf{k}_0 \rangle. \quad (22)$$

The matrix elements of V_Q^S are defined by (17), and are

$$\langle \mathbf{k} \phi_i | V_Q^S | \phi_{i'} \mathbf{k}' \rangle = \langle \mathbf{k} \phi_i | V_1 + (V_{12} + V_Q)[1 + (-1)^S P_r] | \phi_{i'} \mathbf{k}' \rangle + \delta_{ii'} \sum_{\phi_n \in P_1} (\varepsilon_i + \varepsilon_n - E) \langle \mathbf{k} | \phi_n \rangle \langle \phi_n | \mathbf{k}' \rangle. \quad (23)$$

The reduced matrix elements of V_Q have the same form for all one-electron atoms, and are given in Ref. [1].

The Lippmann-Schwinger equation (22) derived here uses plane waves for the projectile $|\mathbf{k}\rangle$. To find the solution of this equation numerically it is often easier to use a distorted-wave representation [6, 25]. This is a purely numerical technique used to minimize the number of integration points necessary to solve this integral equation. It is solved in partial-wave formalism [26] with each partial wave being treated in exactly the same way, with as many partial waves taken as necessary for convergence. The relations between various observables, such as the differential cross section or spin asymmetry, and the partial T -matrix elements, may be found in Ref. [2].

III. DISCUSSION

In Eq. (7) of the preceding section we deliberately split the P and Q spaces so that the former contained only discrete states and the latter only continuum states. In our work preceding Ref. [6] we took Q space to contain not only the continuum but also the higher excited discrete states. These calculations were denoted by $n\text{CCO}$, where n indicated the number of P -space states. The effect of Q -space states was included in all n channels. The contribution of Q -space states on P -space states is calculated in the weak-coupling approximation [1]. By this we mean that only direct coupling between Q - and P -space states is included, with direct coupling between distinct Q -space states being ignored.

In Ref. [6] and subsequent work, we present results of calculations denoted by $m\text{CCO}n$, where now m denotes the number of P -space states, and $n \leq m$ denotes the number of P -space states that have contributions from Q space. As it is the contribution of the continuum part of Q space to the reduced matrix elements of V_Q that take 95% of the calculation time, the calculations $m\text{CCO}n$ and $n\text{CCO}$ take approximately the same time, even if $m \gg n$. The former of these has the advantage that all of the m P -space states are treated via the close-coupling formalism, without having to resort to the weak-coupling approximation.

Using techniques outlined by Bray and Stelbovics [24] we perform a number of $m\text{CC}$ runs, with ever-increasing m until convergence in the particular observable of interest is obtained. This task takes very little time as there is no calculation of the V_Q matrix elements. Having decided on m , we proceed to perform a number of $m\text{CCO}n$ calculations, with ever-increasing n until convergence is obtained. The calculation time grows rapidly with increasing n , but convergence is obtained whenever the observable of interest is contained in the n P -space states.

Convergence studies are channel and energy dependent. For simplicity of presentation, rather than finding the minimum number of m and n necessary for convergence at each energy, we use the same m and n at all energies which yield convergent results at all energies. For the description of the elastic and 2^2P spin asymmetries and differential cross sections up to the $4^2P+4^2D+4^2F$ channel, we take m to be the 13 states in Table I, and n

to be the 8 states that have principle quantum number up to 4 and orbital angular momentum up to 2. In this table we give two sets of energies corresponding to the calculation of the states above the frozen core with (FCHF⁺) and without (FCHF) the phenomenological polarization potential (5). We see that the FCHF model yields quite good one-electron energies, with the FCHF⁺ model providing marginal improvement. Not surprisingly we find that for lithium our results are not significantly affected by either choice of the one-electron wave functions. This is an indication that lithium is the best of the alkali metals for testing scattering theory. Though the lithium target wave functions are not known exactly, as they are for atomic hydrogen, for the purposes of scattering calculations the frozen-core Hartree-Fock model provides an excellent description.

IV. RESULTS

A. Spin asymmetries

If we write the singlet and triplet scattering cross sections as $|S|^2$ and $|T|^2$, respectively, then spin asymmetry A_{ex} is related to the ratio of triplet to singlet scattering $r = |T|^2/|S|^2$ by

$$A_{\text{ex}} = \frac{1-r}{1+3r}. \quad (24)$$

For presentation purposes it has the advantage over r in that it always remain finite: $A_{\text{ex}} = -\frac{1}{3}$ when triplet scattering is dominant ($r = \infty$), and $A_{\text{ex}} = 1$ when singlet scattering is dominant ($r = 0$).

In Fig. 1 we present 13CCO8 and 13CC calculations of the elastic and 2^2P spin asymmetries as a function of energy at the three angles measured by Baum *et al.* [13] (elastic), and Baum *et al.* [14] (inelastic). We see generally very good quantitative agreement of the 13CCO8 calculation and the measurements. By comparing the 13CC and 13CCO8 calculations we see that the target continuum begins to have a significant effect on the spin asymmetries soon after the ionization threshold of 5.4 eV, and yields very good agreement with experiment.

In Fig. 2 the differential spin asymmetries at 5.4, 10, and 20 eV are presented. Comparison of the 13CCO8 and 13CC results show the effect of the continuum on the spin asymmetries as a function of the scattering angle. As expected it is largest for the bigger of the energies presented, and must be treated in order to get agreement with experiment. The measurements are at 65°, 90°, and 107.5°, and have been extracted from Fig. 1.

These two figures indicate that our CCO formalism is valid at low and intermediate energies. As far as we are aware it is the only theory of electron-atom scattering that is able to achieve this result to date. Comparison with some other theories may be found in Refs. [13, 14]. In order to examine some of the small discrepancies between our theory and experiment, e.g., at 90°, it would be helpful to have differential asymmetry measurements at energies around 7 eV. There are no measurements of spin asymmetries at high energies, presumably because

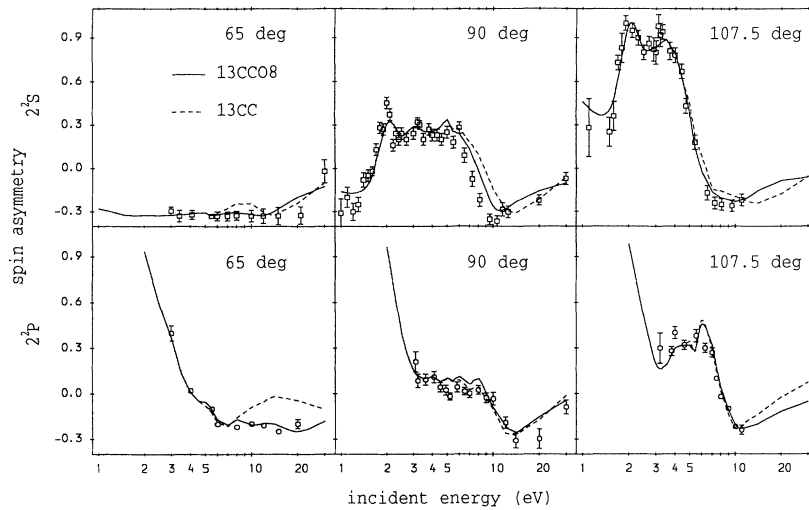


FIG. 1. Spin asymmetries for electron scattering on the ground state of lithium at a range of projectile energies calculated with the 13CCO8 and 13CC models. The 13 states are given in Table I and are sufficient for convergence in the close-coupling expansion using just discrete states. The 13CCO8 calculation has the effect of the continuum target states added to the 8 lowest-lying states via a complex polarization potential. See text for more detail. The measurements are due to Baum *et al.* [13] (elastic) and [14] (inelastic). Quantitative results may be obtained by correspondence with the first author.

they rapidly diminish with increasing energy as exchange becomes less significant.

B. Differential cross sections

The differential cross sections for the elastic, 2^2P , 3^2S , $3^2P + 3^2D$, and $4^2P + 4^2D + 4^2F$ channels at a range of projectile energies incident upon lithium in ground state are presented in this section, and are compared with available measurements. We treat the measurements of Williams, Trajmar, and Bozinis [27] as relative since they give an error of 35% for the integrated cross sections. Accordingly, for graphical presentation we renormalized their data to the integrated cross section of the 13CCO8 results, and compare their estimates of the integrated cross section with the theoretical ones in Table II. The

measurements of Vušković, Trajmar, and Register [28] have errors for the integrated cross sections of 10%, so we treat them as absolute measurements.

In Fig. 3 we present the differential cross sections at 5.4 eV. We see excellent agreement of both the 13CCO8 and 13CC results with the measurements of Williams, Trajmar, and Bozinis [27]. The theoretical integrated cross sections are well within the error bars of their empirical estimates given in Table II. The very small difference between the 13CCO8 and 13CC results indicates that continuum states have little effect on the differential cross sections at this energy. We would expect this since it was also the case for spin asymmetries at this energy.

The differential cross sections at 10 eV are given in Fig. 4. There are considerably more measurements available at this energy. We see generally good agreement between

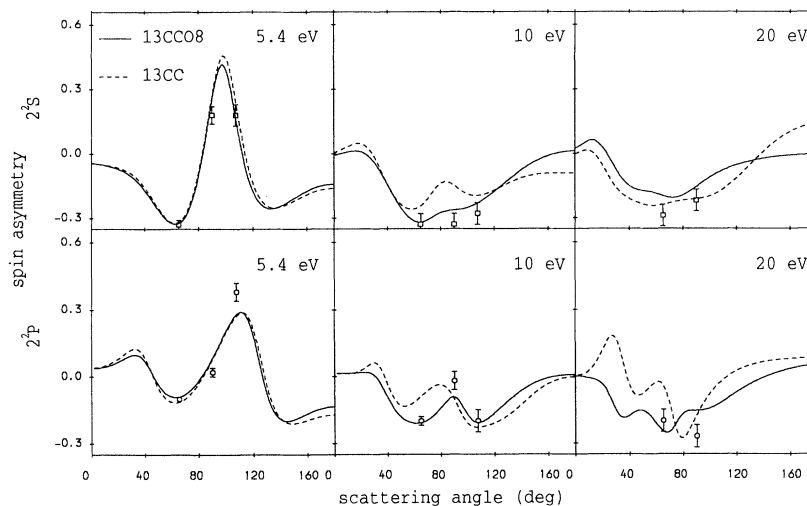


FIG. 2. Differential spin asymmetries for electron scattering on lithium at 5.4-, 10-, and 20-eV projectile energies. The theory and data are as in Fig. 1.

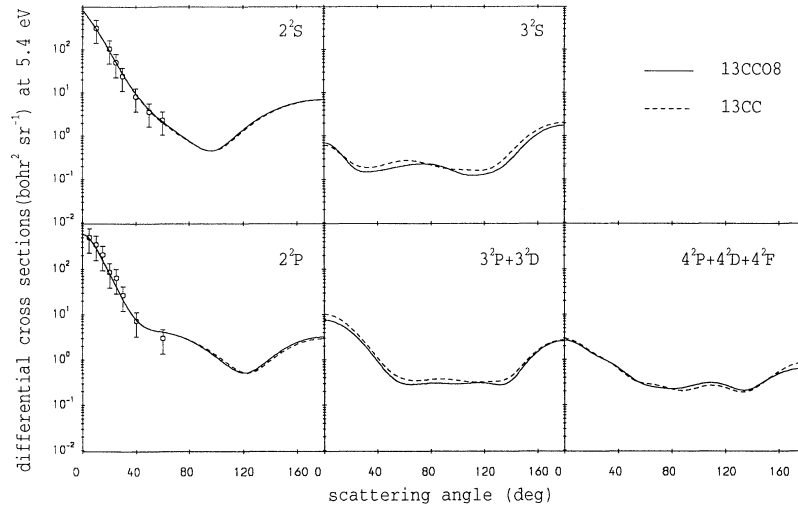


FIG. 3. Differential cross sections for electron scattering on lithium at 5.4-eV projectile energy. The data is due to Williams, Trajmar, and Bozinis [27]. The measurements have been normalized to the 13CCO8 theory (see Fig. 1). Comparison of the theoretical and experimental estimates of the integrated cross sections are in Table II.

theory and experiment. There is a small discrepancy between the measurements of Williams, Trajmar, and Bozinis [27] and Vušković, Trajmar, and Register [28] in the intermediate angular range for the 2^2P channel, with the theory favoring the former. Both sets of measurements and theories yield much the same integrated cross section (after renormalization of the Williams, Trajmar, and Bozinis data) which is dominated by the forward angles, so the discrepancy is not due to normalization. It is an indication of the difficulties associated with mea-

suring the differential cross sections at angles where it has dropped many orders of magnitude from the forward angles. This kind of discrepancy between various measurements is also evident in electron-sodium scattering [4].

Though Williams, Trajmar, and Bozinis [27] claimed to present the differential cross sections for the 3^2P and 4^2P channels, our results indicate that their measurements corresponded to the 3^2P+3^2D and $4^2P+4^2D+4^2F$ channels, respectively. They did specify that they

TABLE II. Integrated cross sections (a_0^2) for electron scattering on lithium. The theoretical results are denoted by 13CCO8. The measurements denoted by Expt. 1, Expt. 2, Expt. 3, Expt. 4 are due to Williams, Trajmar, and Bozinis [27], Vušković, Trajmar, and Register [28], Kasdan, Miller, and Bederson [29], and Jaduszliwer *et al.* [30], respectively.

Channel	Energy	5.4	10	20	60	100	200
		0					
2^2S	13CCO8	149	75.9	39.8	14.8	9.46	5.15
	Expt. 1	175±61	143±50	67.9±24	16.1±6		
2^2P	13CCO8	136	133	109	63.9	42.2	20.8
	Expt. 1	175±61	157±55	129±45	100±35		
	Expt. 2		136±20	111±17	62.5±8	44.3±4	27.0±3
3^2S	13CCO8	3.21	4.50	2.85	1.35	0.89	0.47
	Expt. 1		6.79±2.4	3.93±1.4	3.00±1.1		
3^2P	13CCO8	3.73	3.00	1.56	0.68	0.42	0.20
3^2D	13CCO8	5.30	8.48	6.52	2.84	1.68	0.81
3^2P+3^2D	13CCO8	9.03	11.5	8.08	3.52	2.10	1.01
	Expt. 1		10.7±3.7	9.64±3.4	6.43±2.3		
4^2S	13CCO8	0.58	1.11	0.61	0.31	0.19	0.10
4^2P	13CCO8	1.32	1.27	0.53	0.18	0.11	0.06
4^2D	13CCO8	1.67	2.93	2.05	0.75	0.46	0.22
4^2F	13CCO8	2.06	1.14	0.48	0.12	0.06	0.03
$4^2P+4^2D+4^2F$	13CCO8	5.05	5.34	3.06	1.05	0.63	0.31
	Expt. 1		1.21±0.4	1.79±0.6	1.86±0.6		
σ_t	13CCO8	310	244	169	85.3	54.3	28.0
	Expt. 3	399±48	317±38	236±28	157±19		
	Expt. 4	296±18	257±11				

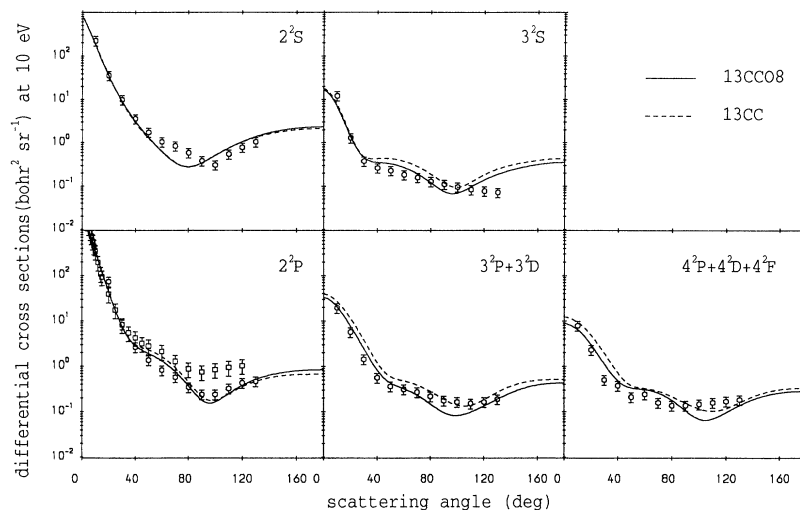


FIG. 4. Differential cross sections for electron scattering on lithium at 10 eV projectile energy. The data denoted by \circ and \square are due to Williams, Trajmar, and Bozinis [27] and Vušković, Trajmar, and Register [28], respectively. The former measurements have been normalized to the 13CC08 theory (see Fig. 1), the latter have not. See text for more detail.

were unable to distinguish between the different channels in each set, but presumed that the P channel was dominant. We find that this is not the case, and in fact it is the D channel that is usually dominant in both sets, see Table II. Without the addition of the other channels, the shape of the theoretical differential cross section would be very different to the measurements.

Comparison of the 13CC08 and 13CC calculations indicates that the continuum does not have a great influence at this energy either. Since we saw in Fig. 2 that the continuum had a significant effect in the 2^2S and 2^2P channels, we conclude that from a theoretical point of view the differential cross section is a considerably less sensitive parameter than the spin asymmetry. Given the

difficulty associated with putting the relative measured differential cross sections on an absolute scale, we see that such measurements are unable to conclusively show that the 13CC08 results are superior to the 13CC ones.

In Fig. 5 we look at the differential cross sections of 20-eV electrons scattering on the ground state of lithium. We see good agreement of the two theories for the 2^2S , 2^2P , and $3^2P + 3^2D$ channels. The remaining two channels show a discrepancy at the forward angles. Given that the results for all channels are calculated simultaneously we are unable to suggest why agreement for some channels would be better than others. This problem appears only at this energy. We see that at 60 eV (Fig. 6) good agreement is again obtained

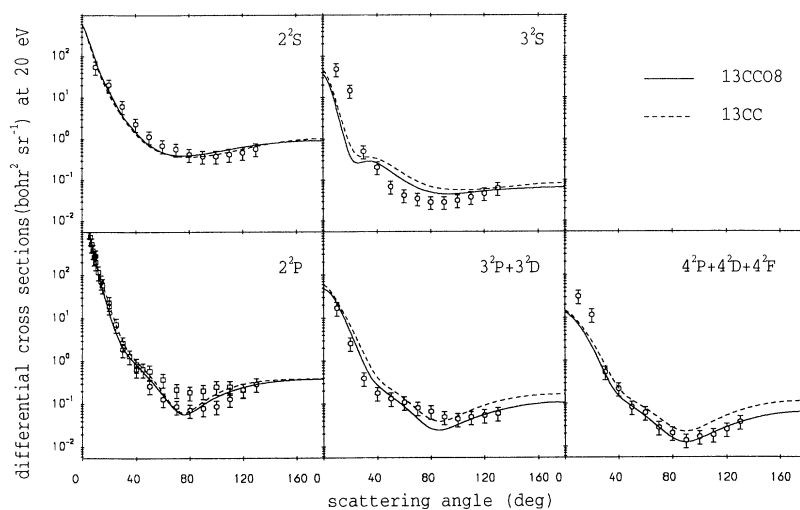


FIG. 5. Differential cross sections for electron scattering on lithium at 20-eV projectile energy. Theory and experiment are the same as for Fig. 4.

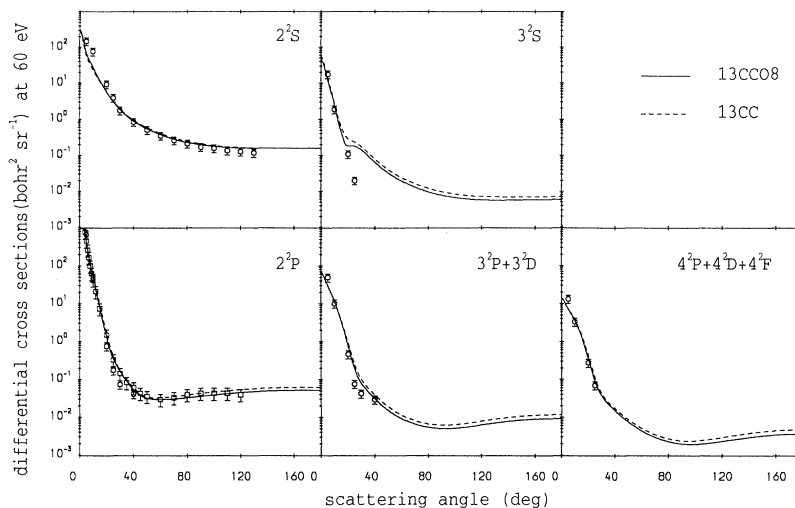


FIG. 6. Differential cross sections for electron scattering on lithium at 60-eV projectile energy. Theory and experiment are the same as for Fig. 4.

for all channels, though it appears that experiment suggests a faster falloff for the 3^2S channel. It is interesting to note that whereas the experiment of Vušković, Trajmar, and Register [28] consistently predicted higher values at the intermediate angles for the 2^2P channel at 10 and 20 eV; it is in excellent agreement with theory at 60 eV.

In Figs. 7 and 8 we present the differential cross sections for projectile energies of 100 and 200 eV, respectively. Only the absolute measurements of Vušković, Trajmar, and Register [28] for the 2^2P channel are available. These are in excellent agreement with theory. Comparison of the 13CCO8 and 13CC results indicates that the already small effect of continuum on the differential cross sections diminishes with increasing energy.

C. Integrated cross sections

In Table II we present our 13CCO8 results of integrated cross sections for the channels considered above, as well as the total cross section. The latter is calculated with the aid of the optical theorem. The integrated cross sections are compared with the estimates of Williams, Trajmar, and Bozinis [27] and Vušković, Trajmar, and Register [28]. We find excellent agreement with the latter estimates for the 2^2P channel at all energies, with the exception of 200 eV. Given the excellent quantitative agreement between their absolute measurements of the differential cross section and our theory (Fig. 8) we are not perturbed by this discrepancy.

For channels with principle quantum number up to

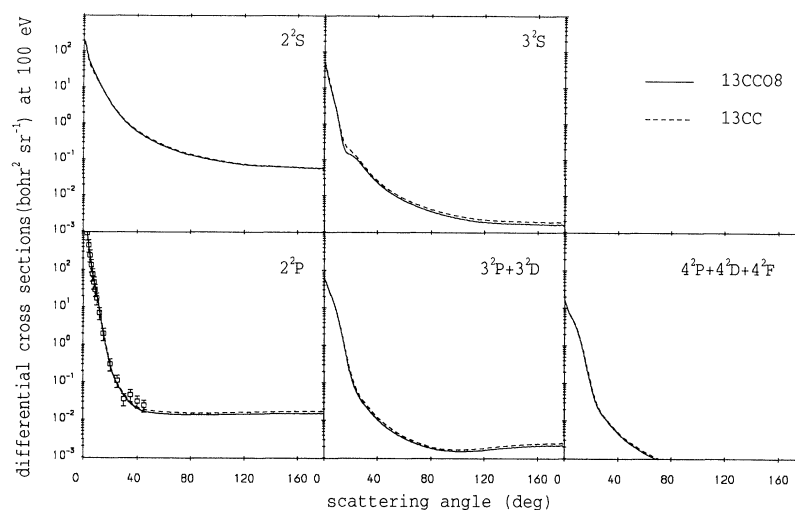


FIG. 7. Differential cross sections for electron scattering on lithium at 100-eV projectile energy. Theory and experiment are the same as for Fig. 4.

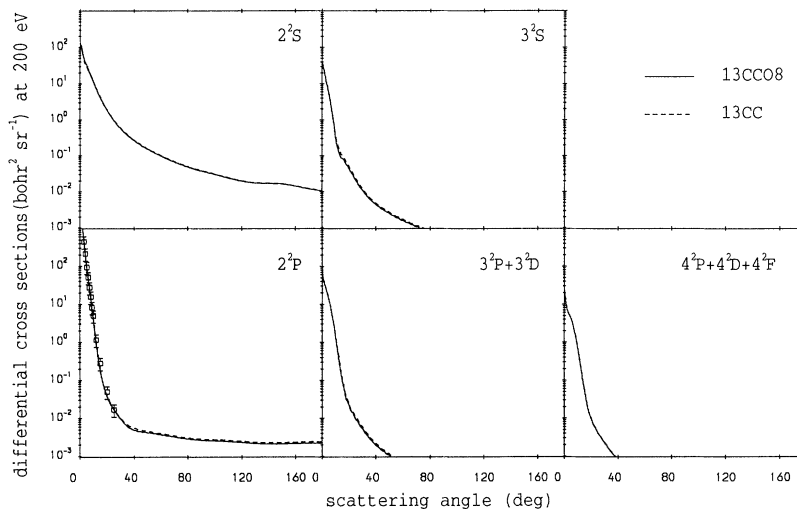


FIG. 8. Differential cross sections for electron scattering on lithium at 200-eV projectile energy. Theory and experiment are the same as for Fig. 4.

3 we are in agreement with the estimates of Williams, Trajmar, and Bozinis, except at 60 eV. At this energy their estimates are consistently higher than our results. Their method of normalization used the measurements of the total cross section of Kasdan, Miller, and Bederson [29]. We see that these are bigger than our results by almost a factor of 2. Given the excellent agreement we have for the 2^2P channel at 60 eV with the measurements of Vušković, Trajmar, and Register, we are confident in the reliability of the cross sections for the other channels.

For the $4^2P + 4^2D + 4^2F$ channel the theoretical results are much higher than experimental estimates of Williams, Trajmar, and Bozinis at 10 and 20 eV, but considerably less at 60 eV. In fact, our results peak at 10 eV and monotonically decrease with increasing energy. The experimental results are monotonically increasing with energy. We suspect that this discrepancy is due to difficulties associated with the method of normalization used in the experiment.

The theoretical total cross section results are consistently below the empirical estimates of Kasdan, Miller, and Bederson [29], but in good agreement with the measurements of Jaduszliwer *et al.* [30]. Given the excellent agreement with recent experiment for the total cross section in electron-sodium scattering [4] we hope that our results for electron scattering on lithium are just as reliable. As the measurements of Kasdan, Miller, and Bederson were utilized in normalizing the experiment of Williams, Trajmar, and Bozinis, this may be one of the reasons for some of the discrepancies between our integrated cross sections and the experimental estimates of Williams, Trajmar, and Bozinis.

V. CONCLUSIONS

We have seen that our CCO theory is able to reproduce measured spin asymmetries and differential cross sections at a large range of energies, with few exceptions. With respect to testing a theory against experiment, a number of factors conspire to make the spin asymmetry measurements more useful. We have seen that the effect of inclusion of the target continuum has a large effect on

the spin asymmetries at intermediate energies, whereas it is less evident on the differential cross sections, and furthermore tends only to lower the cross sections rather than altering their shape. Given the difficulty associated with normalizing measured relative differential cross sections, it is difficult for experiment to differentiate between calculations that do, or do not, treat the target continuum. For theorists normalization is a simple matter, so any theory that is able to get a channel's spin asymmetry is almost guaranteed to get the correct differential cross section as well.

Our results have shown that contrary to the belief of Williams, Trajmar, and Bozinis [27], in the $3^2P + 3^2D$ and $4^2P + 4^2D + 4^2F$ channels it is the d state excitation that is dominant. This is a surprising result, but it is worth noting that the 2^2P channel is by far the most dominant of the inelastic channels.

While we have presented those results of our CCO calculations where there are corresponding measurements, there are many more which have not been presented. The calculations have generated T -matrix elements for the transition from the ground state to any one of the states in Table I at projectile energies of 1 to 200 eV. Upon request, these may be used to obtain observable phenomena of interest to the reader. Any observable phenomena, presented or generated from the stored T -matrix elements, may be obtained by correspondence with the first author.

Having established validity of our CCO theory to electron scattering on hydrogen, lithium, and sodium, we will next turn our attention to electron scattering on potassium. In the course of the present work we found that the role of the phenomenological polarization potential [Eq. (5)] was insignificant for lithium. This will most probably not be the case for the much heavier potassium atom. We plan to investigate the role of structure approximations upon the scattering.

ACKNOWLEDGMENT

We acknowledge support from the Australian Research Council.

- * Electronic address: igor@esm.cc.flinders.edu.au
- [1] I. Bray, D. A. Konovalov, and I. E. McCarthy, Phys. Rev. A **43**, 5878 (1991).
- [2] I. Bray, D. A. Konovalov, and I. E. McCarthy, Phys. Rev. A **44**, 5586 (1991).
- [3] I. Bray, D. A. Konovalov, and I. E. McCarthy, Phys. Rev. A **44**, 7830 (1991).
- [4] I. Bray, D. A. Konovalov, and I. E. McCarthy, Phys. Rev. A **44**, 7179 (1991).
- [5] I. Bray, Phys. Rev. Lett. **69**, 1908 (1992).
- [6] I. Bray and I. E. McCarthy, Phys. Rev. A (to be published).
- [7] J. J. McClelland, M. H. Kelley, and R. J. Celotta, Phys. Rev. A **40**, 2321 (1989).
- [8] J. J. McClelland, S. R. Lorentz, R. E. Scholten, M. H. Kelley, and R. J. Celotta, Phys. Rev. A **46**, 6079 (1992).
- [9] R. E. Scholten, S. R. Lorentz, J. J. McClelland, M. H. Kelley, and R. J. Celotta, J. Phys. B **24**, L653 (1991).
- [10] M. H. Kelley, J. J. McClelland, S. R. Lorentz, R. E. Scholten, and R. J. Celotta, in *Correlations and Polarization in Electronic and Atomic Collisions and ($e,2e$) Reactions*, edited by P. J. O. Teubner and E. Weigold (Institute of Physics, Adelaide, 1992).
- [11] S. R. Lorentz, R. E. Scholten, J. J. McClelland, M. H. Kelley, and R. J. Celotta, Phys. Rev. Lett. **67**, 3761 (1991).
- [12] T. Hegemann, M. Oberste-Vorth, R. Vogts, and G. F. Hanne, Phys. Rev. Lett. **66**, 2968 (1991).
- [13] G. Baum, M. Moede, W. Raith, and U. Sillmen, Phys. Rev. Lett. **57**, 1855 (1986); U. Sillmen, Ph.D. thesis, Bielefeld University, 1989.
- [14] G. Baum, L. Frost, W. Raith, and U. Sillmen, J. Phys. B **22** 1677 (1989); U. Sillmen, Ph.D. thesis, Bielefeld University, 1989.
- [15] P. G. Burke and A. J. Taylor, J. Phys. B **2**, 869 (1969).
- [16] D. L. Moores, J. Phys. B **19**, 1843 (1986).
- [17] M. Kumar, S. S. Tayal, and A. N. Tripathi, J. Phys. B At. Mol. Phys. **18**, 135 (1985).
- [18] T. T. Gien, J. Phys. B **21**, 3767 (1988).
- [19] K. C. Mathur and S. P. Purohit, Phys. Rev. A **42**, 2696 (1990).
- [20] L. V. Chernysheva, N. A. Cherepkov, and V. Radojevic, Comput. Phys. Commun. **11**, 57 (1976).
- [21] L. V. Chernysheva, N. A. Cherepkov, and V. Radojevic, Comput. Phys. Commun. **18**, 87 (1979).
- [22] H. L. Zhou, B. L. Whitten, G. Snitchler, and D. W. Norcross, Phys. Rev. A **42**, 3907 (1990).
- [23] W. Müller, J. Flesch, and W. Meyer, J. Chem. Phys. **80**, 3297 (1984).
- [24] I. Bray and A. T. Stelbovics, Phys. Rev. A **46**, 6995 (1992).
- [25] I. Bray, I. E. McCarthy, J. Mitroy, and K. Ratnavelu, Phys. Rev. A **39**, 4998 (1989).
- [26] I. E. McCarthy and A. T. Stelbovics, Phys. Rev. A **28**, 2693 (1983).
- [27] W. Williams, S. Trajmar, and D. Bozinis, J. Phys. B **9**, 1529 (1976).
- [28] L. Vušković, S. Trajmar, and D. F. Register, J. Phys. B **15**, 2517 (1982).
- [29] A. Kasdan, T. M. Miller, and B. Bederson (unpublished).
- [30] B. Jaduszliwer, A. Tino, B. Bederson, and T. M. Miller, Phys. Rev. A **24**, 1249 (1981).
- [31] C. E. Moore, *Atomic Energy Levels*, Natl. Bur. Stand. (U.S.) Circ. No. 467 (U.S. G.P.O., Washington, D.C., 1949), Vol. 1.